Published in final edited form as:
Neuroscience. 2007 May 25; 146(3): 1232–1244. doi:10.1016/j.neuroscience.2007.01.065.

STATUS EPILEPTICUS CAUSES A LONG-LASTING REDISTRIBUTION OF HIPPOCAMPAL CANNABINOID TYPE 1 RECEPTOR EXPRESSION AND FUNCTION IN THE RAT PILOCARPINE MODEL OF ACQUIRED EPILEPSY

K. W. Falenski[a], **R. E. Blair**[b], **L. J. Sim-Selley**[a], **B. R. Martin**[a], and **R. J. DeLorenzo**[a,b,*]

a*Department of Pharmacology and Toxicology, Virginia Commonwealth University, Richmond, VA 23298, USA*

b*Department of Neurology, Virginia Commonwealth University, PO, Box 980599, Richmond, VA 23298, USA*

Abstract

Activation of the cannabinoid type 1 (CB1) receptor, a major G-protein-coupled receptor in brain, acts to regulate neuronal excitability and has been shown to mediate the anticonvulsant effects of cannabinoids in several animal models of seizure, including the rat pilocarpine model of acquired epilepsy. However, the long-term effects of status epilepticus on the expression and function of the CB1 receptor have not been described. Therefore, this study was initiated to evaluate the effect of status epilepticus on CB1 receptor expression, binding, and G-protein activation in the rat pilocarpine model of acquired epilepsy. Using immunohistochemistry, we demonstrated that status epilepticus causes a unique "redistribution" of hippocampal CB1 receptors, consisting of specific decreases in CB1 immunoreactivity in the dense pyramidal cell layer neuropil and dentate gyrus inner molecular layer, and increases in staining in the CA1-3 strata oriens and radiatum. In addition, this study demonstrates that the redistribution of CB1 receptor expression results in corresponding functional changes in CB1 receptor binding and G-protein activation using [^{3}H] *R*(+)-[2,3-dihydro-5-methyl-3-[(morpholinyl)methyl]pyrrolo [1,2,3-*de*]-1,4-benzoxazin-yl](1-napthalen-yl)methanone mesylate (WIN55,212-2) and agonist-stimulated [^{35}S]GTPγS autoradiography, respectively. The redistribution of CB1 receptor-mediated [^{35}S]GTPγS binding was 1) attributed to an altered maximal effect (E_{max}) of WIN55,212-2 to stimulate [^{35}S]GTPγS binding, 2) reversed by the CB1 receptor antagonist *N*-(piperidin-1-yl)-5-(4-chlorophenyl)-1-(2,4-dichlorophenyl)-4-methyl-1*H*-pyrazole-3-carboxamide hydrochloride (SR141716A), 3) confirmed by the use of other CB1 receptor agonists, and 4) not reproduced in other G-protein-coupled receptor systems examined. These results demonstrate that status epilepticus causes a unique and selective reorganization of the CB1 receptor system that persists as a permanent hippocampal neuronal plasticity change associated with the development of acquired epilepsy.

Keywords

plasticity; G-protein-coupled receptor; immunohistochemistry; [^{35}S]GTPγS autoradiography; [^{3}H] WIN55,212-2 autoradiography; neuroexcitability

*Correspondence to: R. J. DeLorenzo, Department of Neurology, PO, Box 980599, Richmond, VA 23298, USA. Tel: +1-804-828-8969; fax: +1-804-828-6432. E-mail address: rjdelore@vcu.edu (R. J. DeLorenzo).

Status epilepticus (SE) is a major medical and neurological emergency, and is associated with significant morbidity and mortality (DeLorenzo et al., 1996). The injury from SE has been shown to cause epileptogenesis, resulting in acquired epilepsy (AE) (Delorenzo et al., 2005). A number of changes in long-term neuronal plasticity have been observed following SE, including altered excitatory and inhibitory neurotransmission, changes in neurotrophic factors, and reorganization of hippocampal circuitry (Lothman et al., 1991; Morimoto et al., 2004). Recent studies have shown that the endocannabinoid system plays a regulatory role in the suppression of seizure activity (Wallace et al., 2003; Lutz, 2004); thus, a better understanding of the endocannabinoid system following SE may offer important insights into cannabinoid modulation of neuronal excitability.

In the 1970s, cannabinoids were found to be anticonvulsant in several animal models of acute seizure (Karler and Turkanis, 1981), and recently, these anticonvulsant effects have been demonstrated to be cannabinoid type 1 (CB1) receptor-mediated in both *in vivo* and *in vitro* models (Wallace et al., 2001, 2002, 2003; Shafaroodi et al., 2004; Blair et al., 2006). In the rat pilocarpine model of AE, endocannabinoid tone was shown to regulate seizure frequency and duration via a CB1 receptor mechanism (Wallace et al., 2003). The CB1 receptor is among the most abundant G-protein-coupled receptors in brain, and is highly expressed in hippocampus (Herkenham et al., 1991; Tsou et al., 1998), a key region involved in limbic seizure generation (Lothman et al., 1991; Morimoto et al., 2004). Evidence exists that SE induces a long-term alteration in the expression of hippocampal CB1 receptors (Wallace et al., 2003); however, further in depth analysis of regional receptor expression and receptor functionality to determine the effects of SE on plasticity of neuronal CB1 receptors is warranted.

This study was initiated to characterize the long-term effects of SE on CB1 receptor expression, binding, and G-protein activation in the rat pilocarpine model of AE. This model is well-established and manifests many features similar to partial complex or limbic epilepsy in humans (Mello et al., 1993). Utilizing the rat pilocarpine model of SE-induced AE, hippocampal CB1 receptors were evaluated using immunohistochemical and functional autoradiographic assays on brain sections from control and epileptic rats. Immunohistochemical analysis was performed with antibodies directed at two different epitopes of the CB1 receptor. Furthermore, changes in CB1 receptor binding and G-protein activation were evaluated using [^{3}H] *R*(+)-[2,3-dihydro-5-methyl-3-[(morpholinyl)methyl] pyrrolo[1,2,3-*de*]-1,4-benzoxazin-yl](1-napthalen-yl)methanone mesylate (WIN55,212-2) autoradiography (Jansen et al., 1992) and agonist-stimulated [^{35}S]GTPγS autoradiography (Sim et al., 1995), respectively. The results from this study provide the first evidence that SE causes a long-term reorganization in the expression, receptor binding, and G-protein activation of the hippocampal CB1 receptor.

EXPERIMENTAL PROCEDURES

Induction of epilepsy in rats

All animal procedures were approved by the Virginia Commonwealth University IACUC and are in accordance with the NIH Guide for Care and Use of Laboratory Animals. Animal procedures were carried out in a manner to minimize any pain and suffering, and the experimental design was implemented to reduce the number of animals needed. Adult male Sprague–Dawley rats (≈250 g) (Harlan, Indianapolis, IN, USA) were housed in single cages on a 12-h light/dark cycle and were provided with food and water *ad libitum*. The pilocarpine model of epilepsy was used to induce spontaneous recurrent seizures (SRS) after SE by well-established procedures (Mello et al., 1993). Briefly, rats were first administered methyl-scopolamine (1 mg/kg, i.p.) (Sigma, St. Louis, MO, USA) 30 min before treatment to minimize peripheral effects of pilocarpine. Pilocarpine (375 mg/kg, i.p.) (Sigma) was then given to induce SE. Onset of SE was determined by the presence of continuous class 4–5 level seizures

as assessed using the Racine scale (Racine, 1972). Animals undergoing SE were rescued by administration of diazepam (5 mg/kg, i.p.) (VCU Health Systems Pharmacy, Richmond, VA, USA) at 1, 3 and 5 h following SE onset to terminate seizures. Four months following pilocarpine-induced SE, animals were monitored to evaluate the presence of SRS activity. Only pilocarpine-treated rats that had SRSs of levels 4–5 assessed using the Racine scale (Racine, 1972) as observed with 24 h of continuous video recording were determined to be epileptic. Naïve age-matched control and chronically epileptic rats were used for all studies.

Tissue preparation

For immunohistochemical analysis in fixed brain tissue, rats were deeply anesthetized by a ketamine/xylazine cocktail (ketamine/xylazine, 75 mg/7.5 mg/kg, i.p.) (VCU Health Systems Pharmacy) and then briefly flushed transcardially with saline followed by perfusion fixation with 4% paraformaldehyde in a 100 mM sodium phosphate buffer (pH 7.4). Brains were removed and postfixed overnight in the same fixative. The brains were then placed in a 30% sucrose solution in sodium phosphate buffer for cryoprotection and then frozen in isopentane maintained at −30 °C on dry ice. Twenty micrometer coronal sections were cut on a Leitz cryostat (Leica Microsystems, Wetzlar, Germany) maintained at −20 °C and thaw-mounted onto gelatin-subbed slides. Comparable regions of one brain from each experimental condition were placed on the same slide to reduce variability in staining. Slides were stored at −80 °C until use. For [^{3}H]WIN55,212-2 autoradiography and agonist-stimulated [^{35}S]GTPγS autoradiography, rats were briefly anesthetized by halothane (VCU Health Systems Pharmacy) inhalation and killed by rapid decapitation. Brains were quickly removed and frozen in isopentane (Sigma). Coronal sections (20 μm) were cut on a cryostat as described above and collected in triplicate. Slides were stored with desiccant at −80 °C until use.

Immunohistochemical analysis

Immunohistochemistry was performed using polyclonal antibodies generated against either the N-terminus (N-terminus residues 1–77, generously provided by Dr. Ken Mackie, University of Washington) or C-terminus (C-terminus residues 461–473, generously provided by Dr. Maurice Elphick, Queen Mary College) of the CB1 receptor. Immunohistochemistry was performed using modifications of a well-established technique (Tsou et al., 1998). Briefly, sections were incubated in phosphate-buffered saline containing 0.4% Triton X-100 (PBST, 30 min) followed by blocking in SuperBlock Blocking Buffer containing 0.4% Triton X-100 (SBBT, Pierce, Rockford, IL, USA; 1 h). Guinea-pig anti-vesicular GABA transporter (vGAT) (Calbiochem, 2 μg/ml in SBBT, overnight) or rabbit anti-CB1 diluted in SBBT was applied at 1:1000 (72 h) or 1:5000 (1 h) for the N-terminus and C-terminus antibodies, respectively. After 1×5 min SBBT and 3×5 min PBST washes, the sections were incubated in biotinylated anti-rabbit IgG (Vector Laboratories, Burlingame, CA, USA; 1:200 dilution in SBBT, 30 min). Sections were washed as above, then incubated in the avidin– biotin complex (Vector; 1:100 dilution in PBST, 30 min) and visualized using 3′3′-diaminobenzidine peroxidase stain (Vector). The staining reaction was terminated by washing in ddH_2O. Slides were dehydrated in an increasing ethanol gradient, cleared with xylene, and coverslips were mounted using Permount (Fisher Scientific Company, Fair Lawn, NJ, USA). Adjacent sections were Nissl stained. Control experiments included incubation in the absence of primary antibody, as well as coabsorption with an immunizing peptide (N-terminus antibody- 1 μg/ml, C-terminus antibody-20 μM).

Immunofluorescence staining and confocal microscopy

Standard immunohistochemistry and section preparation for analysis of the CB1 receptor was carried out using previously described techniques. Sections were incubated for 1 h in rabbit anti-CB1 (C-terminus, 1:5000). Following 1×5 min SBBT and 3×5 min PBST washes, the

sections were incubated in FITC-conjugated anti-rabbit IgG (Vector Laboratories; 20 μg/ml) diluted in SBBT for 2 h. Labeled sections were washed and slides were coverslipped with Vectashield (Vector) and analyzed by the Leica TCS-SP2 AOBS confocal microscope (Leica Microsystems, Exton, PA, USA). Laser intensity, photo-multiplier gain and offset were held constant throughout each set of experiments. Any signal due to tissue autofluorescence was removed by lambda scanning and subsequent linear unmixing (using Leica TCS-SP2 LCS software). Confocal microscopy images were obtained with a 63× oil HCX Plan Apo objective lens with a theoretical optimum lateral resolution of 139 nm and axial resolution of 236 nm through a 1.4 NA lens, which was adequate to resolve the punctate staining patterns observed with the CB1 receptor antibodies.

[^{3}H]WIN55,212-2 autoradiography

[^{3}H]WIN55,212-2 autoradiography was performed using previously established techniques (Jansen et al., 1992). Briefly, slides were brought to room temperature under cool air and preincubated in assay buffer (20 mM Hepes, 1 mM $MgCl_2$, and 0.5% w/v BSA, pH 7.0) for 20 min at 30 °C. Sections were then incubated in 1 nM [^{3}H]WIN55,212-2 (Perkin-Elmer, Boston, MA, USA: specific activity 40 Ci/mmol) in assay buffer (80 min, 30 °C) in the absence or presence of 1 μM unlabeled WIN55,212-2 to assess total and nonspecific binding, respectively. Sections were then washed in assay buffer (4×10 min, 25 °C) followed by briefly washing in ddH_2O (4 °C). Slides were thoroughly dried overnight and exposed to Kodak Biomax MS film for 4–6 weeks in the presence of ^{3}H microscales (Amersham, Arlington Heights, IL, USA).

Agonist-stimulated [^{35}S]GTPγS autoradiography

Agonist-stimulated [^{35}S]GTPγS autoradiography was carried out according to previously established methods (Sim et al., 1995). Briefly, slides were brought to room temperature, then incubated at 25 °C in assay buffer (50 mM Tris–HCl, 3 mM $MgCl_2$, 0.2 mM EGTA, 100 mM NaCl, and 0.5% BSA, pH 7.4) for 10 min, and transferred to a solution containing 2 mM GDP and 10 mU/ml adenosine deaminase in assay buffer for 20 min. Sections were then incubated for 2 h at 25 °C in 40 pM [^{35}S]GTPγS (Perkin-Elmer: specific activity 1250 Ci/mmol), 2 mM GDP, 10 mU/ml adenosine deaminase, and appropriate ligands to evaluate both CB1 and non-CB1 receptor-mediated G-protein activation. These included maximally effective concentrations of the CB1 receptor agonists WIN55,212-2 (10 μM), (−)-*cis*-3-[2-hydroxy-4-(1,1-dimethylheptyl)phenyl]-*trans*-4-(3-hydroxypropyl)cyclohexanol (CP55, 940; 3 μM) (Sigma), or methanandamide (10 μM) (NIDA Chemical Synthesis and Drug Supply Program); non-CB1 G-protein-coupled receptor agonists included [D-Ala(2),N-MePhe(4),Glyol(5)] enkephalin (DAMGO; 10 μM) (Sigma) for μ opioid, phenylisopropyladenosine (PIA; 10 μM) (Sigma) for adenosine A_1, sphingosine-1-phosphate (S1P; 50 μM) (Sigma) for S1P, or baclofen (300 μM) (Sigma) for $GABA_B$ receptors. Additional assays included varying concentrations of WIN55,212-2 (0.03, 0.1, 0.5, 1.0, 5.0, and 10.0 μM) (Sim-Selley and Martin, 2002), or WIN55,212-2 (1.0 μM) in the presence or absence of *N*-(piperidin-1-yl)-5-(4-chlorophenyl)-1-(2,4-dichlorophenyl)-4-methyl-1*H*-pyrazole-3-carboxamide hydrochloride (SR141716A) (0.3 μM) (NIDA Chemical Synthesis and Drug Supply Program). Basal binding was assessed in the absence of agonist. Slides were rinsed in 50 mM Tris at 4 °C (2×2 min each) and ddH_2O at 4 °C (30 s), dried overnight, and exposed to Kodak Biomax MR film with ^{14}C microscales (Amersham). Films were developed after a 24 h exposure. The same slides were then Nissl stained for anatomical identification of regions of interest, and images were overlaid using Adobe Photoshop®.

Data analysis

Brain sections processed using immunohistochemistry were evaluated using a binocular microscope and photographed using a digital camera (Olympus Inc., Melville, NY, USA). All camera settings including exposure time, gain, and offset were held constant throughout capturing. Digitized images were analyzed and densitometrically quantitated using Analysis® software (Soft Imaging System, Lakewood, CO, USA) and Scion Image for Windows (Scion Corporation, Frederick, MD, USA). For densitometric analysis of CB1 receptor and vGAT-immunostained sections, selected hippocampal regions (including CA1 stratum pyramidale, CA3 stratum radiatum, CA3 stratum oriens, and dentate gyrus inner molecular layer) from four to five animals per group were evaluated. Following acquisition of high-resolution digitized grayscale images, mean pixel intensity per area (0–255) above background were measured for each circled region and averaged across both hemispheres. For CA1 pyramidal cell counts of dorsal hippocampus in adjacent Nissl-stained sections, high-resolution digitized images were acquired for measurement. Neurons with clearly identified nuclei were counted and compared between control and epileptic animals, and data were expressed as % control values.

Analysis of sections processed in agonist-stimulated [^{35}S]GTPγS autoradiography and [^{3}H] WIN55,212-2 autoradiography was conducted as previously described (Sim-Selley and Martin, 2002). Briefly, analysis was performed using NIH Image and Microsoft Excel. Autoradiographic images were quantified by densitometric analysis with either [^{14}C] or [^{3}H] microscale standards, and values were corrected to nanocuries/gram [^{35}S] and nanocuries/milligram [^{3}H] as previously described (Jansen et al., 1992; Sim et al., 1995). Graphs and concentration-effect curves were plotted using Sigma Plot 5.0. Data are reported as means ±SEM of triplicate sections. Net [^{35}S]GTPγS binding is defined as (agonist-stimulated [^{35}S] GTPγS binding–basal [^{35}S]GTPγS binding). Maximal effect (E_{max}) and EC_{50} values of concentration effect curves were estimated by JMP statistical software, version 2.0.5 (SAS Institute, Inc., Cary, NC, USA). Specific [^{3}H]WIN55,212-2 binding is defined as (total [^{3}H] WIN55,212-2 binding–nonspecific [^{3}H]WIN55,212-2 binding). The unpaired Student's *t*-test was used to evaluate differences between control and epileptic groups.

RESULTS

Redistribution of hippocampal CB1 receptor expression following SE in the pilocarpine model of AE

To thoroughly evaluate the distribution of CB1 receptor expression in the hippocampus and control for specificity, we employed immunohistochemical analysis using antibodies to both the N and C-termini of the CB1 receptor. Animals exposed to SE that later developed SRS activity were employed as epileptic animals and compared with control animals. In tissue from age-matched control rats, the N-terminus antibody used in this study produced a distribution of hippocampal CB1 receptor immunoreactivity similar to what has been previously reported (Tsou et al., 1998), while changes in several regions throughout the hippocampus are evident in epileptic animals (Fig. 1). Fig. 1A presents representative low-magnification images of CB1 receptor immunoreactivity from control and epileptic hippocampi demonstrating the SE induced chronic changes in CB1 receptor expression. These changes represent a long-lasting reorganization of hippocampal CB1 receptor immunoreactivity following SE and are evident by increased receptor expression in the strata radiatum, lacunosum-moleculare and oriens regions surrounding the full length of the stratum pyramidale (CA1-4), while a dropout in expression is observed within the stratum pyramidale of CA1-3 and the inner molecular layer of the dentate gyrus.

Higher magnification of CB1 receptor immunoreactivity further elucidated the SE-induced reorganization in brain tissue. Control tissue manifested intense CB1 receptor expression

surrounding the pyramidal cell layer in a band of staining in the stratum pyramidale throughout CA1 (Fig. 1B) and CA3 (Fig. 1C). In epileptic animals, however, this dense network of CB1 receptor immunoreactivity was virtually absent in the CA1-3 pyramidal cell layer of the hippocampus (Fig. 1B and C). Analysis of Nissl-stained serial sections from control and epileptic animals was performed (Fig. 1B and C), revealing a decrease in CA1 pyramidal cell counts of 11.7%±7.1% in epileptic animals, consistent with what our laboratory has been previously reported in this model (Rice and DeLorenzo, 1998). In CB1 receptor-immunostained control tissue, the strata radiatum, lacunosum-moleculare, and oriens of CA1-3, as well as in the CA4-hilar region revealed fine networks of fibers that were faintly immunopositive, but were less intense than what was observed in the stratum pyramidale. In contrast, in epileptic animals, the intensity of this CB1 receptor immunoreactivity in these strata was increased dramatically without significant changes in morphology in Nissl-stained sections (Fig. 1B, C, D). In the dentate gyrus of control animals, the molecular layer exhibited high CB1 receptor-immunoreactivity, with the densest staining within the inner third (inner molecular layer) bordering the immunonegative granule cell layer (Fig. 1D). In epileptic animals, however, immunostaining of the inner molecular layer was markedly reduced while staining of the outer molecular layer of the dentate gyrus was elevated (Fig. 1D).

The C-terminus antibody produced a similar distribution of CB1 receptor immunostaining in control brain as that observed with the N-terminus antibody, the major exception being the lack of any neuronal somatic staining, as previously reported (Egertova and Elphick, 2000) (Fig. 2). In hippocampi of epileptic animals, the C-terminus antibody staining showed a distribution comparable with immunostaining observed using the N-terminus antibody, with decreases in CB1 receptor-immunoreactivity in the CA1 stratum pyramidale (Fig. 2A), and increases in CA1-3 strata oriens, lacunosum-moleculare, radiatum and the CA4-hilar area (Fig. 2A, B). In the dentate gyrus, the epileptic animals demonstrated lower CB1 receptor-immunoreactivity in the inner molecular layer and increased immunoreactivity in the outer molecular layers (Fig. 2C), similar to the N-terminus antibody.

To obtain high-resolution analysis of CB1 receptor expression in control and epileptic hippocampi, confocal immunofluorescence microscopy was performed on the stratum pyramidale and stratum radiatum (Fig. 3 and 4). Under higher magnification, the pyramidal cells in control tissue were immunonegative, but were surrounded by a very dense fiber plexus with punctate CB1 receptor immunoreactivity (Fig. 3C). Studies have shown that the majority of CB1 receptors in this region are localized to GABAergic presynaptic terminals that surround the principal cell somata of CA1–CA3 (Tsou et al., 1999;Hajos et al., 2000;Katona et al., 1999;Hoffman and Lupica, 2000). In hippocampi of epileptic animals, however, the characteristic CB1 receptor staining surrounding the pyramidal cell somata was dramatically reduced (Fig. 3D). Conversely, in the stratum radiatum, fine networks of fibers with CB1 immunoreactivity were increased in epileptic animals when compared with controls (Fig. 4A, B). At higher magnification, the increased CB1 immunoreactivity in the stratum radiatum appeared to be due to increased punctate staining (Fig. 4C, D) and may therefore be associated with presynaptic CB1 localization in these regions.

Densitometric analysis of CB1 receptor immunoreactivity in several discrete hippocampal regions was performed to substantiate the qualitative immunohistochemical analysis. Representative regions illustrating increases or decreases in CB1 receptor immunoreactivity as observed in Fig. 5A, B were selected for quantitation (see Experimental Procedures), and analysis of the cerebellum molecular layer was also included as a control. The CA1 stratum pyramidale and dentate gyrus inner molecular layer in hippocampi from epileptic animals exhibited significant decreases in CB1 immunoreactivity of 47±11% and 46±8% respectively when compared with age-matched control (Fig. 5C), while the CA3 strata radiatum and oriens increased by 60±18% and 62±17% respectively (Fig. 5C), without significant alterations in

immunoreactivity in the cerebellum. To evaluate if SE has long-term effects on the level of GABAergic terminals surrounding the stratum pyramidale somata, immunohistochemistry was also conducted using an antibody to vGAT, the presynaptic vesicular GABAergic transporter. Consistent with a recent report (Kwak et al., 2006), vGAT staining in the CA1 stratum pyramidale in epileptic rats was not significantly altered (93.9±8.2% of control, *n*=5) in the hippocampus following pilocarpine-induced SE.

Collectively, these results demonstrate that SE induced a long-term redistribution of CB1 receptor expression in the hippocampus, with decreases in CB1 receptor-immunoreactivity in the dentate gyrus inner molecular layer and the stratum pyramidale of CA1-3, and concurrent increases in CB1 receptor immunostaining in the strata radiatum and oriens of CA1–CA4, without changes in the cerebellum molecular layer. In our hands, we observe a marginal decrease in CA1 pyramidal cell counts following SE that agrees with previous findings from our laboratory (Rice and DeLorenzo, 1998). In addition, we observe no difference in vGAT immunoreactivity surrounding CA1 pyramidal somata between epileptic and age-matched controls. These findings suggest that neither a decrease in cell number nor loss in presynaptic GABAergic innervation can fully account for the loss observed in CB1 receptor immunoreactivity surrounding the stratum pyramidale somata following SE induced AE (Fig. 1B).

[^{3}H]WIN55,212-2 binding is altered in hippocampi of epileptic animals

To determine whether redistribution of CB1 receptor expression is associated with a change in CB1 receptor binding, [^{3}H]WIN55,212-2 autoradiography was performed in brain slices from age-matched control and epileptic rats. [^{3}H]WIN55,212-2 binding in control brain was similar to previous reports using [^{3}H]-CP55,940 autoradiography, which showed high levels of [^{3}H]-CP55,940 binding in the dentate gyrus molecular layer, the stratum lacunosum-moleculare, and in narrow bands flanking the pyramidal cell layer (Herkenham et al., 1991) (Fig. 6A). However, epileptic animals exhibited a pattern of [^{3}H]WIN55,212-2 binding that was remarkably similar to the distribution shown in the immunohistochemical studies (Fig. 6B). [^{3}H]WIN55,212-2 binding was increased in the strata radiatum and oriens for CA1–CA4. Conversely, [^{3}H]WIN55, 212-2 binding was decreased in the stratum pyramidale and the inner molecular layer of the dentate gyrus compared with control.

To quantitate the reorganization of [^{3}H]WIN55,212-2 binding, densitometric analysis of [^{3}H] WIN55,212-2 autoradiographs was employed. [^{3}H]WIN55,212-2 binding in the whole hippocampus revealed that epileptic animals exhibited significantly increased [^{3}H] WIN55,212-2 binding when compared with control, without changes in nonspecific binding (Fig. 6C). Further densitometric analysis of [^{3}H]WIN55,212-2 binding in more discrete regions of hippocampi revealed significant increases in [^{3}H]WIN55,212-2 binding in the stratum radiatum and significant decreases in the stratum pyramidale and dentate gyrus inner molecular layer in epileptic animals when compared with control, without changes in the cerebellum molecular layer (Fig. 6C).

CB1 receptor-mediated G-protein activity measured by [^{35}S]GTPγS autoradiography exhibits redistribution in epileptic rats

To determine whether changes in CB1 receptor expression and binding resulted in parallel functional changes in G-protein activation, agonist-stimulated [^{35}S]GTPγS autoradiography was employed in hippocampi from age-matched control and epileptic animals. The distribution of WIN55,212-2 stimulated [^{35}S]GTPγS binding in control hippocampi was similar to previous [^{35}S]GTPγS studies (Fig. 7A) (Sim et al., 1995). In contrast, WIN55,212-2 stimulated [^{35}S] GTPγS binding in hippocampi from epileptic rats exhibited changes that correlated with the redistribution in both protein expression and [^{3}H]WIN55,212-2 autoradiography (Fig. 7B).

Fig. 7B demonstrates that SE caused a long-lasting increase in WIN55,212-2 stimulated [^{35}S]GTPγS binding in the strata radiatum and oriens of CA1-3, and a chronic decrease in WIN55,212-2 stimulated [^{35}S]GTPγS binding in the CA1–CA3 pyramidal cell layer and dentate gyrus inner molecular layer.

To quantitate the reorganization of WIN55,212-2 stimulated [^{35}S]GTPγS binding, densitometric analysis of [^{35}S]GTPγS autoradiography was employed. Densitometric analysis of whole hippocampus revealed significant increases in WIN55,212-2 stimulated [^{35}S]GTPγS binding in brains from epileptic versus control rats (Fig. 7C, Table 1). Densitometric analysis of specific regions within the hippocampus revealed significant increases in WIN55,212-2-stimulated [^{35}S]GTPγS binding in the stratum radiatum, and conversely showed significant decreases in the dentate gyrus inner molecular layer (Fig. 7C, Table 1) in hippocampi from epileptics compared with controls, without changes in the cerebellum. Basal binding did not differ significantly between control and epileptic animals for any of the regions analyzed (controls versus epileptics: 237±6 vs. 241±10 in whole hippocampus, 269±7 vs. 278 ±12 in the CA3 stratum radiatum, 106±15 vs. 128±13 for the CA1 stratum pyramidale, and 258±9 vs. 249±10 in the dentate gyrus inner molecular layer, n=9–10 per group, unpaired Student's t-test). Addition of the CB1 receptor antagonist SR141716A completely reduced WIN55,212-2-stimulated [^{35}S]GTPγS binding to basal levels in control and epileptic whole hippocampi and stratum radiatum (Table 1). This inhibition occurred at concentrations of WIN55,212-2 high enough to produce ≈80–90% of its E_{max} (Sim et al., 1995). Furthermore, SR141716A alone did not produce any significant decreases in [^{35}S]GTPγS binding from basal values in control or epileptic tissue (Table 1).

Agonist-stimulated [^{35}S]GTPγS binding was also performed using CB1 receptor agonists CP55,940 and methanandamide, both of which stimulated [^{35}S]GTPγS binding in a distribution comparable to WIN55,212-2 in control and epileptic animals (data not shown). Methanandamide acted as a partial agonist, producing approximately 50% of the [^{35}S]GTPγS binding seen with high efficacy agonists WIN55,212-2 and CP55,940 (Selley et al., 2001). Densitometric analysis revealed that methanandamide- and CP55,940-stimulated [^{35}S]GTPγS binding were significantly increased in the hippocampus and stratum radiatum of epileptic animals when compared with controls (Table 1), similar to WIN55,212-2. CP55,940-stimulated [^{35}S]GTPγS binding was also significantly decreased in the dentate gyrus inner molecular layer of epileptic animals (Table 1).

Concentration-effect curves were generated in the hippocampus for control and epileptic animals to determine whether changes in WIN55,212-2-stimulated [^{35}S]GTPγS binding resulted from a change in the E_{max} (efficacy) or EC_{50} (potency) of WIN55,212-2 to activate CB1 receptors (Fig. 8). The E_{max} for WIN55,212-2 to stimulate [^{35}S]GTPγS binding in whole hippocampus and CA3 stratum radiatum was significantly increased in hippocampi from epileptics when compared with controls (Table 2). Analysis of the dentate gyrus inner molecular layer in epileptic tissue, however, resulted in a significantly lower E_{max} value (Table 2), and only analysis of this region revealed a significantly decreased EC_{50} value for WIN55,212-2 in epileptics compared with controls (Table 2). These data demonstrate that increases in WIN55,212-2-stimulated [^{35}S]GTPγS binding in epileptics are due to regions that have greater E_{max} rather than a change in CB1 receptor affinity for WIN55,212-2, and may therefore be the result of activation of a greater number of receptors.

Effect of SE on other G-protein-coupled receptor activity as measured by agonist-stimulated [^{35}S]GTPγS autoradiography

To compare CB1 receptor agonist-stimulated [^{35}S]GTPγS binding that occurs in epileptic animals to that of other G-protein-coupled receptor systems, agonist-stimulated [^{35}S]GTPγS binding was conducted to evaluate μ opioid, adenosine A_1, S1P and $GABA_B$ G-protein-coupled

receptor activity. In age-matched control rats, the distribution of each of these G-protein-coupled receptor systems was consistent with previous reports (Sim et al., 1995; Waeber and Chiu, 1999; Moore et al., 2000); in epileptics, the distribution of agonist-stimulated [^{35}S]GTPγS binding for these receptor systems was similar to control (data not shown). Densitometric analysis of agonist-stimulated [^{35}S]GTPγS binding in the stratum radiatum elucidated significant increases only in WIN55,212-2- and baclofen ($GABA_B$)-stimulated [^{35}S]GTPγS binding in epileptic animals; conversely, analysis of the dentate gyrus inner molecular layer resulted in only a decrease in WIN55,212-2-stimulated [^{35}S]GTPγS binding (Table 1). Therefore, in these analyzed regions, only CB1 receptor G-protein activation exhibits a robust redistribution in the hippocampus following SE in the G-protein-coupled receptor systems analyzed.

DISCUSSION

This study elucidates a unique plasticity of the endocannabinoid system that occurs within the hippocampus following SE in the pilocarpine model of AE. The results indicate that there are not merely changes in CB1 receptor expression levels, but that a reorganization of CB1 receptor protein expression occurs in discrete hippocampal regions. The changes in CB1 receptor expression included selective decreases in the stratum pyramidale of CA1–CA3 and the dentate gyrus inner molecular layer, with concomitant increases in the strata radiatum and oriens. In addition, this study demonstrated using [^{3}H]WIN55,212-2 autoradiography and agonist-stimulated [^{35}S]GTPγS autoradiography that this CB1 receptor redistribution resulted in corresponding changes in CB1 receptor binding sites and G-protein activation. The long-term changes in WIN55,212-2-stimulated [^{35}S]GTPγS binding following SE were likely the result of altered CB1 receptor expression, and not due to alterations in putative additional cannabinoid receptors, because similar findings were seen with other CB1 receptor agonists, the effects were reversed by SR14716A, and the redistribution was not replicated in other G-protein-coupled receptor systems examined. The results of this study provide the first direct evidence that SE produces a long-term reorganization in both hippocampal CB1 receptor expression and function, and suggest that this redistribution may play an important role in the permanent plasticity changes associated with brain injury from SE and epileptogenesis.

It was important to evaluate whether SE caused redistribution in the activity of other hippocampal G-protein-coupled receptors. Therefore, this study evaluated several other major G-protein-coupled receptor systems following SE utilizing agonist-stimulated [^{35}S]GTPγS autoradiography. Besides WIN55,212-2-stimulated [^{35}S]GTPγS binding, only baclofen-stimulated [^{35}S]GTPγS binding significantly increased in the CA3 stratum radiatum in epileptic animals compared with controls (Table 2). This finding is consistent with studies where kindling induced long-lasting increases in $GABA_B$ receptor immunoreactivity in the piriform cortex (Kokaia and Kokaia, 2001), and where upregulation of $GABA_B$ receptor mRNA and protein expression occurred following kainite-induced SE (Furtinger et al., 2003) (reviewed in Morimoto et al., 2004). Other G-protein-coupled receptor systems have also been studied in epilepsy models; activation of the adenosine A_1 receptor has been shown to modulate excitability (reviewed in Boison, 2005), and activation of the G-protein-coupled receptor S1P was recently hypothesized to correlate with the onset of seizure activity (MacLennan et al., 2001). In our studies, PIA-stimulated (adenosine A_1 receptor) and S1P-stimulated (S1P receptor) [^{35}S]GTPγS binding showed a trend for increased [^{35}S]GTPγS binding in whole hippocampus and stratum radiatum of epileptic animals, but were not significantly altered in any region (Table 2). The results indicate that while these other G-protein-coupled receptor systems may be undergoing long term neuronal plasticity changes in this model, under conditions where SE caused significant reorganization of CB1 receptor function, these other G-protein-coupled receptor systems were not significantly affected. Thus, the effect of SE on the long-term reorganization of the CB1 receptor is both novel and selective.

Evidence from our study suggests that the loss in CB1 receptor immunoreactivity surrounding the CA1 stratum pyramidale in pilocarpine-induced AE is due to a selective loss in CB1 receptors on GABAergic inputs to the pyramidal cells. Pilocarpine-induced SE has been shown to cause varying degrees of hippocampal neuronal loss, including the CA1 stratum pyramidale (Mello et al., 1993; Rice and DeLorenzo, 1998). Our findings only showed a marginal degree of CA1 pyramidal cell loss. Furthermore, there were no significant changes in basal [^{35}S]GTPγS binding values in this region compared with control, which would have been affected with dramatic cell loss. The marginal hippocampal cell loss observed in the present study could perhaps be attributed to differences in strain, or the rigorous administration of diazepam to rescue the animal and minimize neuronal injury while still producing AE. In addition, CB1 receptors are highly expressed in the neuropil surrounding the principal cell somata of CA1–CA3 and studies have demonstrated that this localization is primarily on presynaptic GABAergic terminals (Tsou et al., 1999; Hajos et al., 2000) where receptor activation can modulate GABA release (Katona et al., 1999; Hajos et al., 2000; Hoffman and Lupica, 2000). Using confocal analysis, our findings were in agreement with these studies revealing punctate staining surrounding the stratum pyramidale indicative of GABAergic synapses. Furthermore, our results show no change in vGAT immunoreactivity following SE in agreement with a previous study (Kwak et al., 2006), suggesting that GABAergic terminals in the CA1 region remain intact in epileptic animals. Thus, the observed decrease in staining throughout the pyramidal cell layer following SE may therefore represent a compensatory neuronal plasticity mechanism to allow for increased GABAergic input onto pyramidal cells, decreasing overall CNS excitability.

The CB1 receptor has also recently been localized to glutamatergic terminals, albeit at much lower levels than on GABAergic terminals (Marsicano and Lutz, 1999; Katona et al., 2006; Kawamura et al., 2006), and CB1 receptor activation inhibits glutamate release in several paradigms (Shen et al., 1996; Ameri et al., 1999; Misner and Sullivan, 1999; Ameri and Simmet, 2000). Our confocal studies demonstrated a marked increase in staining in the stratum radiatum following SE that appears punctate in nature. Such a reorganization of CB1 receptor expression could act as a compensatory mechanism to regulate excessive glutamate release known to occur in the epileptic brain (Sherwin, 1999). Interestingly, the anticonvulsant effect of endocannabinoid uptake inhibitor UCM707 in the kainic acid model of seizure is mediated specifically by CB1 receptors on glutamatergic neurons (Marsicano et al., 2003). The more precise localization of these receptor changes to symmetric or asymmetric synapses could be addressed by future studies at confocal and EM levels.

Recent evidence has pointed to the existence of additional cannabinoid receptor subtypes in the hippocampus that mediate inhibition of glutamate (Hajos et al., 2001; Hajos and Freund, 2002a; Hoffman et al., 2003, 2005). Additionally, WIN55,212-2 was shown to act at non-CB1 receptors through its ability to stimulate [^{35}S]GTPγS binding in brains of CB1 receptor (−/−) mice (Breivogel et al., 2001). However, several lines of evidence suggest that the cannabinoid receptor redistribution seen in hippocampi of epileptic animals is CB1 receptor-mediated and not due to changes in expression or activation of an uncharacterized cannabinoid receptor subtype. First, CP55,940, which does not significantly stimulate [^{35}S]GTPγS binding in CB1 receptor (−/−) mice (Breivogel et al., 2001), produced the same redistribution of CB1 receptor mediated G-protein activation in the epileptic brain as WIN55,212-2. Furthermore, SR141716A completely inhibited WIN55,212-2-stimulated [^{35}S]GTPγS binding in epileptic animals to basal levels. Additionally, the N-terminus antibody used in this study has been previously characterized and illustrates negligible staining in CB1 receptor (−/−) mice (Hajos et al., 2000).

Recent findings have suggested that the endocannabinoid modulation of glutamatergic transmission in forebrain (Domenici et al., 2006) and hippocampus (Takahashi and Castillo,

2006) is due to the presence of CB1 receptors on glutamatergic terminals. In the hippocampus, depolarization-induced suppression of excitation (DSE) can be induced with longer depolarizations (Ohno-Shosaku et al., 2002), which, like depolarization-induced suppression of inhibition, may not be common under normal physiological conditions (Hampson et al., 2003), but potentially exists during epileptic discharges. This DSE was also shown to be CB1 receptor specific, as it was not seen in CB1 (−/−) mice (Ohno-Shosaku et al., 2002). It is therefore possible that a compensatory recruitment of DSE in epileptic animals may occur, resulting in reducing the spread of excitation among pyramidal cells during epileptic seizures (Hajos and Freund, 2002b).

The long-term plasticity of CB1 receptors in the pilocarpine model is different from the acute effects of hyperthermia-induced seizures on CB1 expression, where the hippocampal pattern of CB1 receptor immunoreactivity did not change, but qualitatively appeared stronger (Chen et al., 2003). However, the parameters of this study were quite different, including the method used to induce seizures, the age of the animals, seizure severity, and the duration between seizure induction and kill. The results of this paper demonstrate an essentially permanent change in receptor plasticity, and we have previously shown this to occur up to 1 year post-SE (Wallace et al., 2003). Additionally, the pilocarpine model of AE uses an injury from SE to induce epileptogenesis, and the effects of SE-induced epileptogenesis on neuronal plasticity have been shown to be very different from single seizures (Lothman et al., 1991; Delorenzo et al., 2005). This study elucidates important effects of SE in causing an essentially permanent change in the CB1 G-protein-coupled receptor system in brain that has important implications in mediating some of the pathophysiology of epilepsy.

This study has broad implications for the function of the endocannabinoid system in modulating neuronal excitability, particularly as a mechanism to control seizures in epileptic animals. These findings demonstrate a capability of the brain endocannabinoid system to undergo compensatory changes following SE that act to maximize an anticonvulsant effect of endogenously released cannabinoids and ultimately minimize seizure activity. The alterations in CB1 receptors in response to SE injury represent a major long-term neuronal plasticity change in the hippocampus. Understanding the role of these plasticity changes in the endocannabinoid system may provide important insights into the pathophysiology of epileptogenesis. The CB1 receptor and endocannabinoid system may therefore represent a target for novel agents to control epileptic seizures and prevent epileptogenesis.

Abbreviations

AE, acquired epilepsy
CB1, cannabinoid type 1
CP55, 940, (−)-*cis*-3-[2-hydroxy-4-(1,1-dimethylheptyl)phenyl]-*trans*-4-(3-hydroxypropyl) cyclohexanol
DSE, depolarization-induced suppression of excitation
E_{max}, maximal effect
PBST, phosphate-buffered saline containing 0.4% Triton X-100
PIA, phenylisopropyladenosine
SBBT, SuperBlock Blocking Buffer containing 0.4% Triton X-100
SE, status epilepticus
SRS, spontaneous recurrent seizure
SR141716A, *N*-(piperidin-1-yl)-5-(4-chlorophenyl)-1-(2,4-dichlorophenyl)-4-methyl-1*H*-pyrazole-3-carboxamide hydrochloride
S1P, sphingosine-1-phosphate
vGAT, vesicular GABA transporter

WIN55, 212-2, *R*(+)-[2,3-dihydro-5-methyl-3-[(morpholinyl)methyl]pyrrolo[1,2,3-*de*]-1,4-benzoxazin-yl](1-napthalen-yl)methanone mesylate

Acknowledgments

This work was supported by the National Institute of Drug Abuse of the National Institutes of Health grants DA05274, DA07027, and DA14277 as well as RO1-NS23350 and P50-NS25630, and the National Institute of Neurological Disorders and Stroke, grant R01-NS052529.

The authors would like to gratefully thank Drs. Ken Mackie (DA11322 awarded to Ken Mackie) and Maurice Elphick (Wellcome Trust grant 057058 awarded to Maurice Elphick, Queen Mary, University of London, UK) for providing their antisera and Dr. Scott Henderson for assistance with confocal microscopy; confocal microscopy was performed at the Virginia Commonwealth University Department of Anatomy and Neurobiology Microscopy Facility, supported, in part, by NIH-NINDS Center core grant 5P30NS047463. The authors would also like to thank Elisa Atkisson for technical assistance.

REFERENCES

Ameri A, Simmet T. Effects of 2-arachidonylglycerol, an endogenous cannabinoid, on neuronal activity in rat hippocampal slices. Naunyn Schmiedebergs Arch Pharmacol 2000;361:265–272. [PubMed: 10731038]

Ameri A, Wilhelm A, Simmet T. Effects of the endogenous cannabinoid, anandamide, on neuronal activity in rat hippocampal slices. Br J Pharmacol 1999;126:1831–1839. [PubMed: 10372827]

Blair RE, Deshpande LS, Sombati S, Falenski KW, Martin BR, Delorenzo RJ. Activation of the CB1 receptor mediates the anticonvulsant properties of cannabinoids in the hippocampal neuronal culture models of acquired epilepsy and status epilepticus. J Pharmacol Exp Ther 2006;317:1072–1078. [PubMed: 16469864]

Boison D. Adenosine and epilepsy: from therapeutic rationale to new therapeutic strategies. Neuroscientist 2005;11:25–36. [PubMed: 15632276]

Breivogel CS, Griffin G, Di Marzo V, Martin BR. Evidence for a new G protein-coupled cannabinoid receptor in mouse brain. Mol Pharmacol 2001;60:155–163. [PubMed: 11408610]

Chen K, Ratzliff A, Hilgenberg L, Gulyas A, Freund TF, Smith M, Dinh TP, Piomelli D, Mackie K, Soltesz I. Long-term plasticity of endocannabinoid signaling induced by developmental febrile seizures. Neuron 2003;39:599–611. [PubMed: 12925275]

Delorenzo RJ, Sun DA, Deshpande LS. Cellular mechanisms underlying acquired epilepsy: the calcium hypothesis of the induction and maintenance of epilepsy. Pharmacol Ther 2005;105:229–266. [PubMed: 15737406]

DeLorenzo RJ, Hauser WA, Towne AR, Boggs JG, Pellock JM, Penberthy L, Garnett L, Fortner CA, Ko D. A prospective, population-based epidemiologic study of status epilepticus in Richmond, Virginia. Neurology 1996;46:1029–1035. [PubMed: 8780085]

Domenici MR, Azad SC, Marsicano G, Schierloh A, Wotjak CT, Dodt HU, Zieglgansberger W, Lutz B, Rammes G. Cannabinoid receptor type 1 located on presynaptic terminals of principal neurons in the forebrain controls glutamatergic synaptic transmission. J Neurosci 2006;26:5794–5799. [PubMed: 16723537]

Egertova M, Elphick MR. Localisation of cannabinoid receptors in the rat brain using antibodies to the intracellular C-terminal tail of CB. J Comp Neurol 2000;422:159–171. [PubMed: 10842224]

Furtinger S, Bettler B, Sperk G. Altered expression of GABAB receptors in the hippocampus after kainic-acid-induced seizures in rats. Brain Res Mol Brain Res 2003;113:107–115. [PubMed: 12750012]

Hajos N, Freund TF. Pharmacological separation of cannabinoid sensitive receptors on hippocampal excitatory and inhibitory fibers. Neuropharmacology 2002a;43:503–510. [PubMed: 12367597]

Hajos N, Freund TF. Distinct cannabinoid sensitive receptors regulate hippocampal excitation and inhibition. Chem Phys Lipids 2002b;121:73–82. [PubMed: 12505692]

Hajos N, Ledent C, Freund TF. Novel cannabinoid-sensitive receptor mediates inhibition of glutamatergic synaptic transmission in the hippocampus. Neuroscience 2001;106:1–4. [PubMed: 11564411]

Hajos N, Katona I, Naiem SS, MacKie K, Ledent C, Mody I, Freund TF. Cannabinoids inhibit hippocampal GABAergic transmission and network oscillations. Eur J Neurosci 2000;12:3239–3249. [PubMed: 10998107]

Hampson RE, Zhuang SY, Weiner JL, Deadwyler SA. Functional significance of cannabinoid-mediated, depolarization-induced suppression of inhibition (DSI) in the hippocampus. J Neurophysiol 2003;90:55–64. [PubMed: 12649318]

Herkenham M, Lynn AB, Johnson MR, Melvin LS, de Costa BR, Rice KC. Characterization and localization of cannabinoid receptors in rat brain: a quantitative in vitro autoradiographic study. J Neurosci 1991;11:563–583. [PubMed: 1992016]

Hoffman AF, Lupica CR. Mechanisms of cannabinoid inhibition of GABA(A) synaptic transmission in the hippocampus. J Neurosci 2000;20:2470–2479. [PubMed: 10729327]

Hoffman AF, Riegel AC, Lupica CR. Functional localization of cannabinoid receptors and endogenous cannabinoid production in distinct neuron populations of the hippocampus. Eur J Neurosci 2003;18:524–534. [PubMed: 12911748]

Hoffman AF, Macgill AM, Smith D, Oz M, Lupica CR. Species and strain differences in the expression of a novel glutamate-modulating cannabinoid receptor in the rodent hippocampus. Eur J Neurosci 2005;22:2387–2391. [PubMed: 16262678]

Jansen EM, Haycock DA, Ward SJ, Seybold VS. Distribution of cannabinoid receptors in rat brain determined with aminoalkylin-doles. Brain Res 1992;575:93–102. [PubMed: 1504787]

Karler R, Turkanis SA. The cannabinoids as potential antiepileptics. J Clin Pharmacol 1981;21:437S–448S. [PubMed: 6975285]

Katona I, Sperlagh B, Sik A, Kafalvi A, Vizi ES, Mackie K, Freund TF. Presynaptically located CB1 cannabinoid receptors regulate GABA release from axon terminals of specific hippocampal interneurons. J Neurosci 1999;19:4544–4558. [PubMed: 10341254]

Katona I, Urban GM, Wallace M, Ledent C, Jung KM, Piomelli D, Mackie K, Freund TF. Molecular composition of the endocannabinoid system at glutamatergic synapses. J Neurosci 2006;26:5628–5637. [PubMed: 16723519]

Kawamura Y, Fukaya M, Maejima T, Yoshida T, Miura E, Watanabe M, Ohno-Shosaku T, Kano M. The CB1 cannabinoid receptor is the major cannabinoid receptor at excitatory presynaptic sites in the hippocampus and cerebellum. J Neurosci 2006;26:2991–3001. [PubMed: 16540577]

Kokaia Z, Kokaia M. Changes in GABAB receptor immunoreactivity after recurrent seizures in rats. Neurosci Lett 2001;315:85–88. [PubMed: 11711221]

Kwak SE, Kim JE, Kim DS, Won MH, Lee HJ, Choi SY, Kwon OS, Kim JS, Kang TC. Differential paired-pulse responses between the CA1 region and the dentate gyrus are related to altered CLC-2 immunoreactivity in the pilocarpine-induced rat epilepsy model. Brain Res 2006;1115:162–168. [PubMed: 16930566]

Lothman EW, Bertram EH 3rd, Stringer JL. Functional anatomy of hippocampal seizures. Prog Neurobiol 1991;37:1–82. [PubMed: 1947175]

Lutz B. On-demand activation of the endocannabinoid system in the control of neuronal excitability and epileptiform seizures. Biochem Pharmacol 2004;68:1691–1698. [PubMed: 15450934]

MacLennan AJ, Carney PR, Zhu WJ, Chaves AH, Garcia J, Grimes JR, Anderson KJ, Roper SN, Lee N. An essential role for the H218/AGR16/Edg-5/LP(B2) sphingosine 1-phosphate receptor in neuronal excitability. Eur J Neurosci 2001;14:203–209. [PubMed: 11553273]

Marsicano G, Lutz B. Expression of the cannabinoid receptor CB1 in distinct neuronal subpopulations in the adult mouse forebrain. Eur J Neurosci 1999;11:4213–4225. [PubMed: 10594647]

Marsicano G, Goodenough S, Monory K, Hermann H, Eder M, Cannich A, Azad SC, Cascio MG, Gutierrez SO, Van Der Stelt M, Lopez-Rodriguez ML, Casanova E, Schutz G, Zieglgansberger W, Di Marzo V, Behl C, Lutz B. CB1 cannabinoid receptors and on-demand defense against excitotoxicity. Science 2003;302:84–88. [PubMed: 14526074]

Mello LE, Cavalheiro EA, Tan AM, Kupfer WR, Pretorius JK, Babb TL, Finch DM. Circuit mechanisms of seizures in the pilocarpine model of chronic epilepsy: cell loss and mossy fiber sprouting. Epilepsia 1993;34:985–995. [PubMed: 7694849]

Misner DL, Sullivan JM. Mechanism of cannabinoid effects on long-term potentiation and depression in hippocampal CA1 neurons. J Neurosci 1999;19:6795–6805. [PubMed: 10436037]

Moore RJ, Xiao R, Sim-Selley LJ, Childers SR. Agonist-stimulated [35S]GTPgammaS binding in brain modulation by endogenous adenosine. Neuropharmacology 2000;39:282–289. [PubMed: 10670423]

Morimoto K, Fahnestock M, Racine RJ. Kindling and status epilepticus models of epilepsy: rewiring the brain. Prog Neurobiol 2004;73:1–60. [PubMed: 15193778]

Ohno-Shosaku T, Tsubokawa H, Mizushima I, Yoneda N, Zimmer A, Kano M. Presynaptic cannabinoid sensitivity is a major determinant of depolarization-induced retrograde suppression at hippocampal synapses. J Neurosci 2002;22:3864–3872. [PubMed: 12019305]

Racine RJ. Modification of seizure activity by electrical stimulation. II. Motor seizure. Electroencephalogr Clin Neurophysiol 1972;32:281–294. [PubMed: 4110397]

Rice AC, DeLorenzo RJ. NMDA receptor activation during status epilepticus is required for the development of epilepsy. Brain Res 1998;782:240–247. [PubMed: 9519269]

Selley DE, Rorrer WK, Breivogel CS, Zimmer AM, Zimmer A, Martin BR, Sim-Selley LJ. Agonist efficacy and receptor efficiency in heterozygous CB1 knockout mice: relationship of reduced CB1 receptor density to G-protein activation. J Neurochem 2001;77:1048–1057. [PubMed: 11359870]

Shafaroodi H, Samini M, Moezi L, Homayoun H, Sadeghipour H, Tavakoli S, Hajrasouliha AR, Dehpour AR. The interaction of cannabinoids and opioids on pentylenetetrazole-induced seizure threshold in mice. Neuropharmacology 2004;47:390–400. [PubMed: 15275828]

Shen M, Piser TM, Seybold VS, Thayer SA. Cannabinoid receptor agonists inhibit glutamatergic synaptic transmission in rat hippocampal cultures. J Neurosci 1996;16:4322–4334. [PubMed: 8699243]

Sherwin AL. Neuroactive amino acids in focally epileptic human brain: a review. Neurochem Res 1999;24:1387–1395. [PubMed: 10555779]

Sim LJ, Selley DE, Childers SR. In vitro autoradiography of receptor-activated G proteins in rat brain by agonist-stimulated guanylyl 5′-[gamma-[35S]thio]-triphosphate binding. Proc Natl Acad Sci U S A 1995;92:7242–7246. [PubMed: 7638174]

Sim-Selley LJ, Martin BR. Effect of chronic administration of R-(+)-[2,3-dihydro-5-methyl-3-[(morpholinyl)methyl]pyrrolo[1,2,3-de]-1,4-b enzoxazinyl]-(1-naphthalenyl)methanone mesylate (WIN55,212-2) or delta(9)-tetrahydrocannabinol on cannabinoid receptor adaptation in mice. J Pharmacol Exp Ther 2002;303:36–44. [PubMed: 12235230]

Takahashi KA, Castillo PE. The CB1 cannabinoid receptor mediates glutamatergic synaptic suppression in the hippocampus. Neuroscience 2006;139:795–802. [PubMed: 16527424]

Tsou K, Mackie K, Sanudo-Pena MC, Walker JM. Cannabinoid CB1 receptors are localized primarily on cholecystokinin-containing GABAergic interneurons in the rat hippocampal formation. Neuroscience 1999;93:969–975. [PubMed: 10473261]

Tsou K, Brown S, Sanudo-Pena MC, Mackie K, Walker JM. Immunohistochemical distribution of cannabinoid CB1 receptors in the rat central nervous system. Neuroscience 1998;83:393–411. [PubMed: 9460749]

Waeber C, Chiu ML. In vitro autoradiographic visualization of guanosine-5′-O-(3-[35S]thio)triphosphate binding stimulated by sphingosine 1-phosphate and lysophosphatidic acid. J Neurochem 1999;73:1212–1221. [PubMed: 10461914]

Wallace MJ, Martin BR, DeLorenzo RJ. Evidence for a physiological role of endocannabinoids in the modulation of seizure threshold and severity. Eur J Pharmacol 2002;452:295–301. [PubMed: 12359270]

Wallace MJ, Wiley JL, Martin BR, DeLorenzo RJ. Assessment of the role of CB1 receptors in cannabinoid anticonvulsant effects. Eur J Pharmacol 2001;428:51–57. [PubMed: 11779037]

Wallace MJ, Blair RE, Falenski KW, Martin BR, DeLorenzo RJ. The endogenous cannabinoid system regulates seizure frequency and duration in a model of temporal lobe epilepsy. J Pharmacol Exp Ther 2003;307:129–137. [PubMed: 12954810]

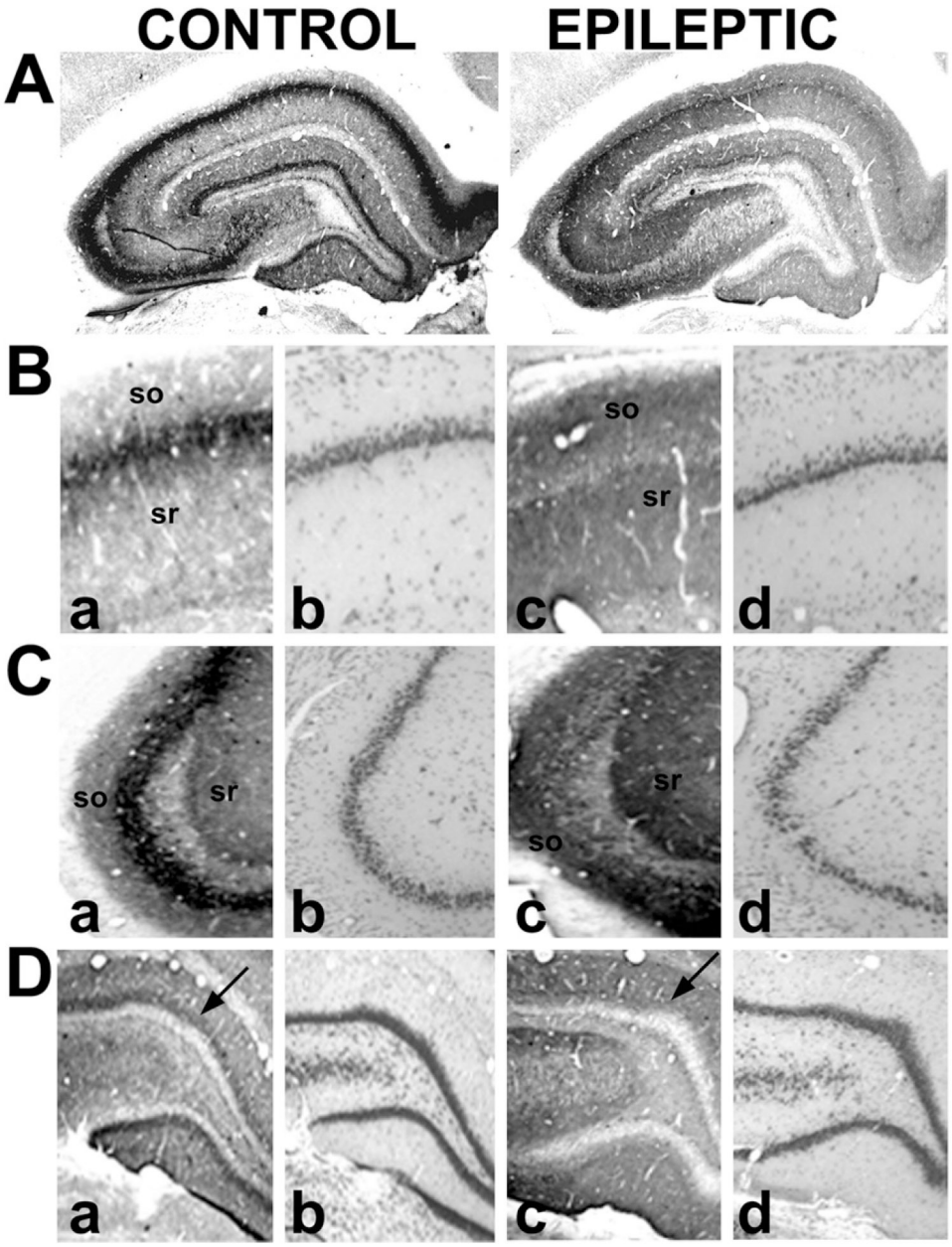

Fig. 1.

Immunohistochemical detection of CB1 receptor expression in hippocampi from control and epileptic rats using an antibody to the N-terminus (N-terminus residues 1–77). Representative contrast-enhanced images of CB1 immunoreactivity (A) of control and epileptic hippocampi. Higher magnification images of CA1 (B), CA3 (C), and the dentate gyrus (D) in control (a, b) and epileptic (c, d) animals. Nissl stains ([B–D]b, [B–D]d) were evaluated in adjacent sections. In comparison to controls, epileptic animals illustrated increased staining in the stratum radiatum (sr), stratum oriens (so), CA4-hilar region, and the outer molecular layer of the dentate gyrus, and decreased staining in both the neuropil on the pyramidal layer of CA1-3 and the inner molecular layer of the dentate gyrus (arrows).

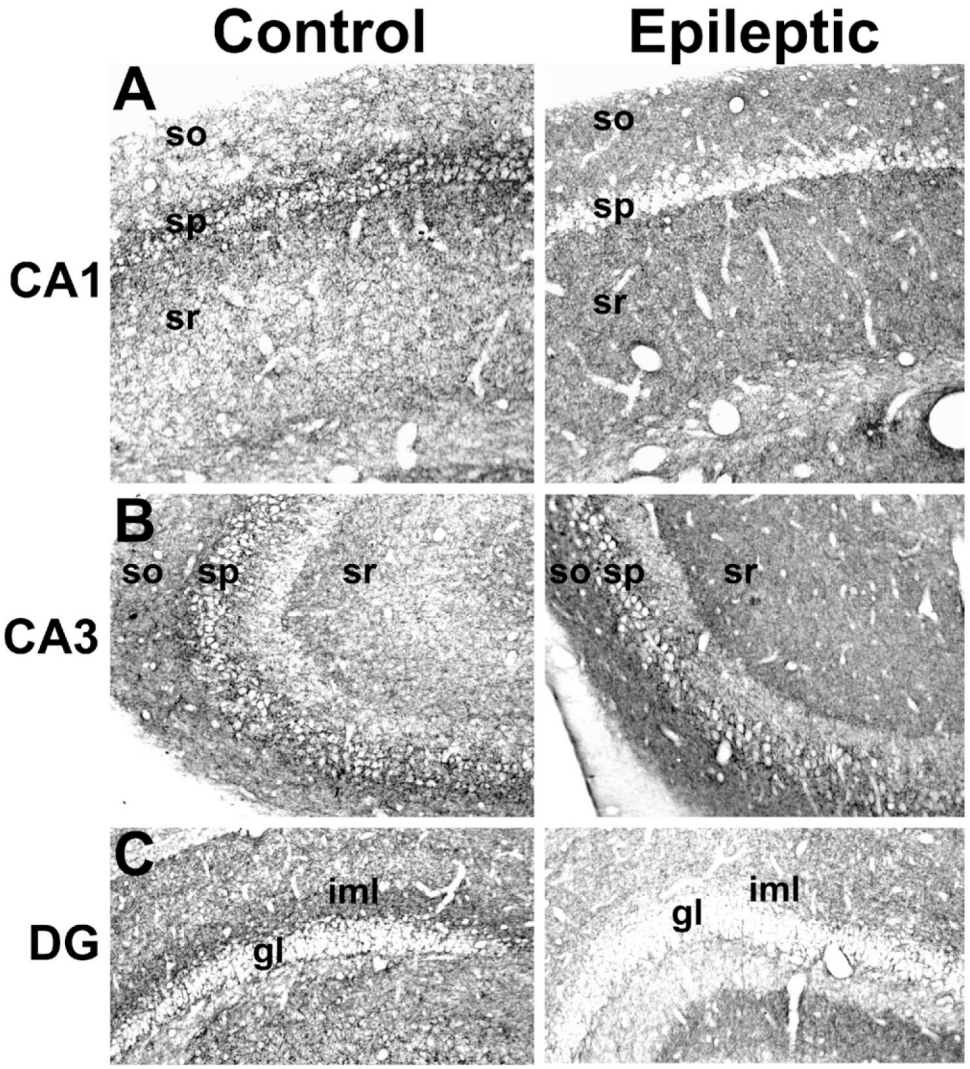

Fig. 2.

Immunohistochemical detection of CB1 receptor expression in hippocampi from control and epileptic rats using an antibody to C-terminus residues 461–473. Representative images of CA1 (top panels), CA3 (middle panels), and the dentate gyrus (lower panels) in hippocampi from control (left) and epileptic (right) animals. Epileptic animals demonstrated increased CB1-receptor immunoreactivity in the dendritic layers surrounding the stratum pyramidale (sp), including the stratum radiatum (sr) and stratum oriens (so), throughout the hippocampus. However, epileptics displayed decreased staining in the pyramidal cell layer, and in the dentate gyrus inner molecular layer (iml) (gl, granule cell layer).

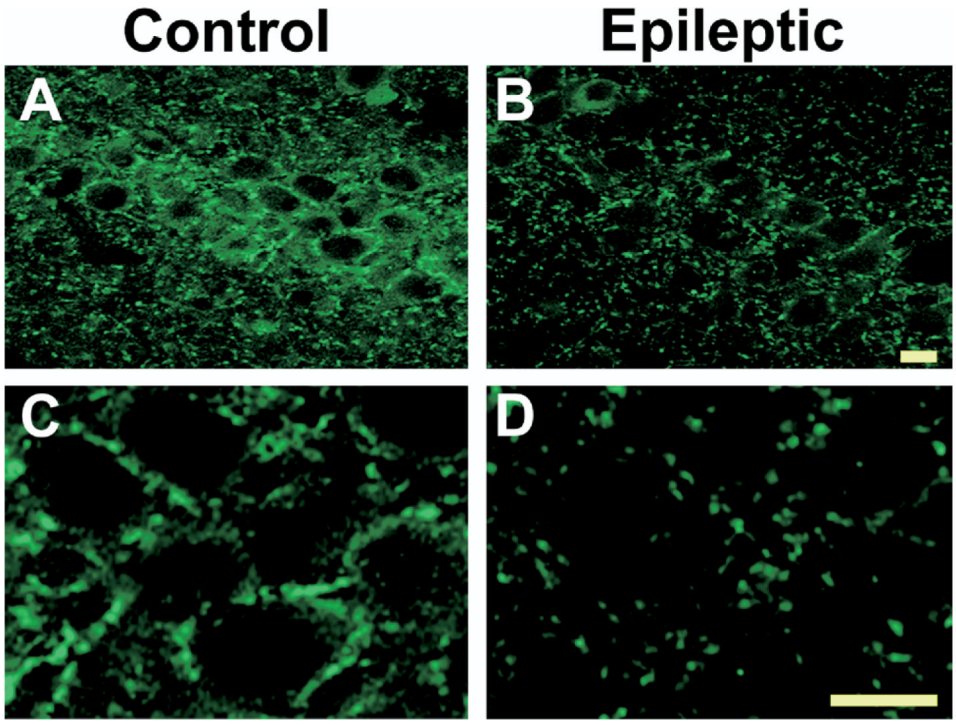

Fig. 3.

High-resolution confocal immunofluorescent detection of CB1 receptor expression in CA1 stratum pyramidale in hippocampi from control and epileptic rats using the C-terminus antibody. Representative images of CA1 at low (A, B) and high (C, D) magnification. Epileptic animals displayed decreased staining in the neuropil surrounding the pyramidal cell layer (scale=10 μm).

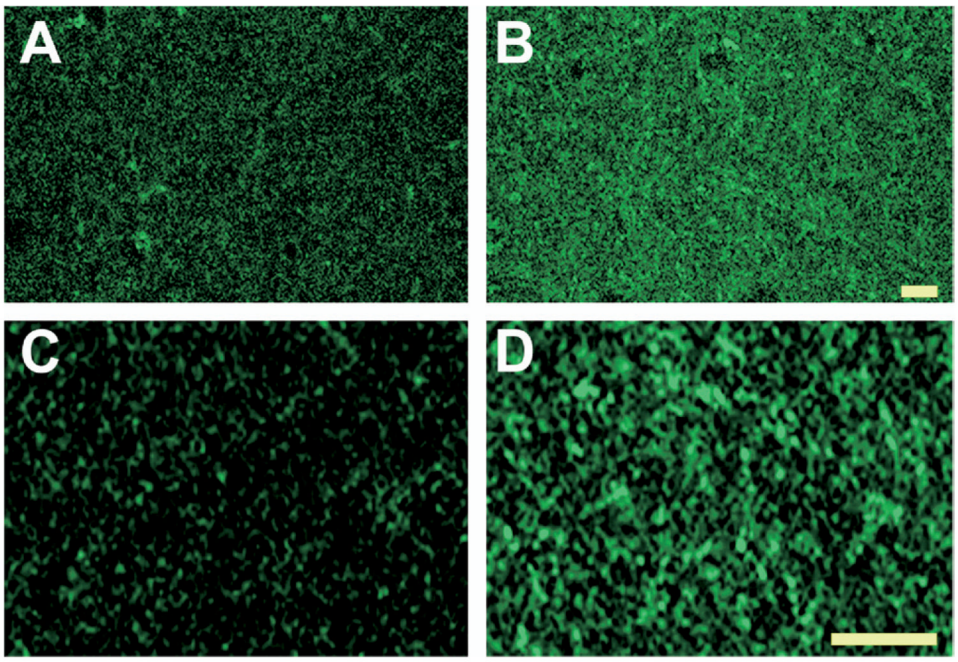

Fig. 4.

High-resolution confocal immunofluorescent detection of CB1 receptor expression in CA3 stratum radiatum from control and epileptic rats using an antibody to C-terminus. Representative images of CA3 at low (A, B) and high (C, D) magnification (scale=10 μm).

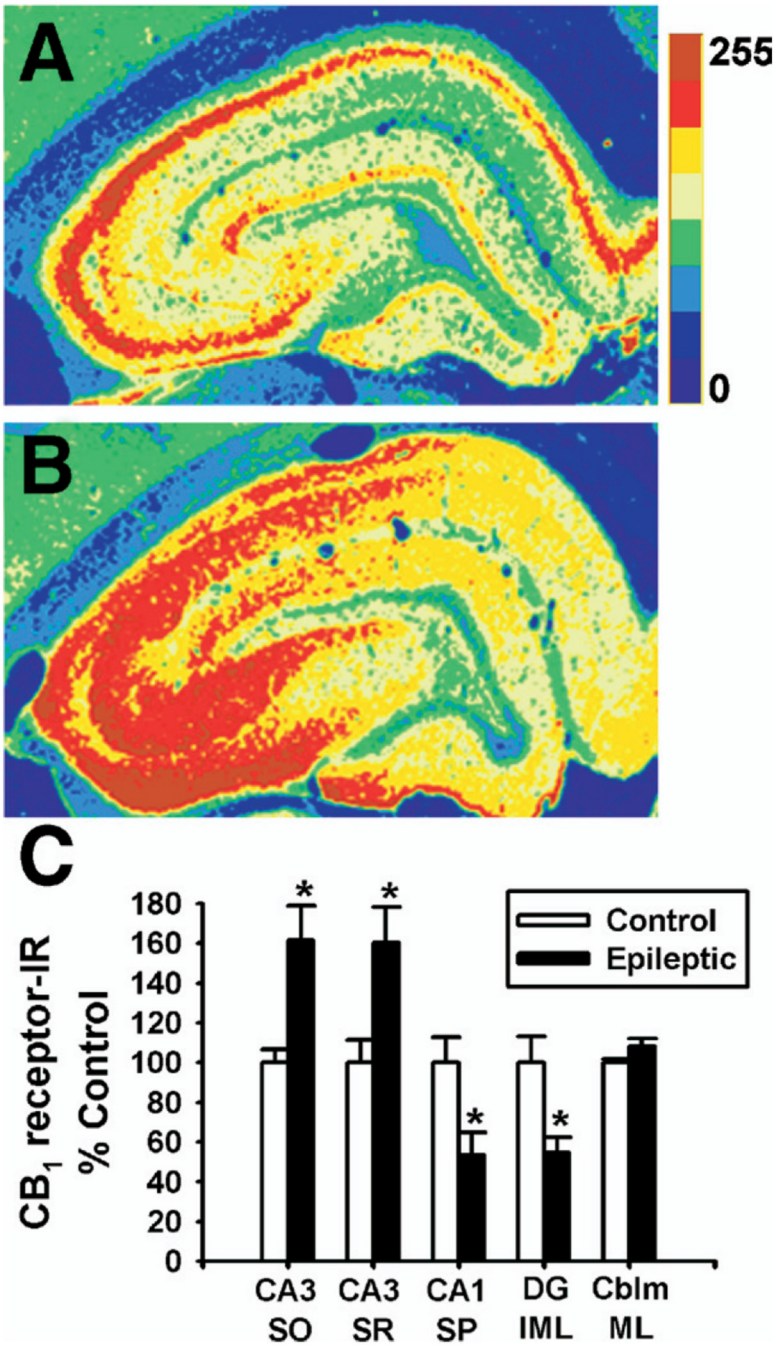

Fig. 5.

Densitometric analysis of CB1 receptor-immunoreactivity in hippocampi from control and epileptic rats. Immunohistochemistry using the N-terminus antibody was evaluated. Representative pseudocolor-enhanced immunoreactivity of control (A) and epileptic (B) hippocampi. The color scale bar represents pixel intensity (0–255) with blue being lowest, and maroon highest. (C) Hippocampal regions analyzed included the CA3 stratum oriens (CA3 SO) and stratum radiatum (CA3 SR), as well as the stratum pyramidale at CA1 (CA1 SP) and the dentate gyrus inner molecular layer (DG IML). The cerebellum molecular layer was also evaluated as a negative control (n=4 per group, Student's t-test, * P<0.05).

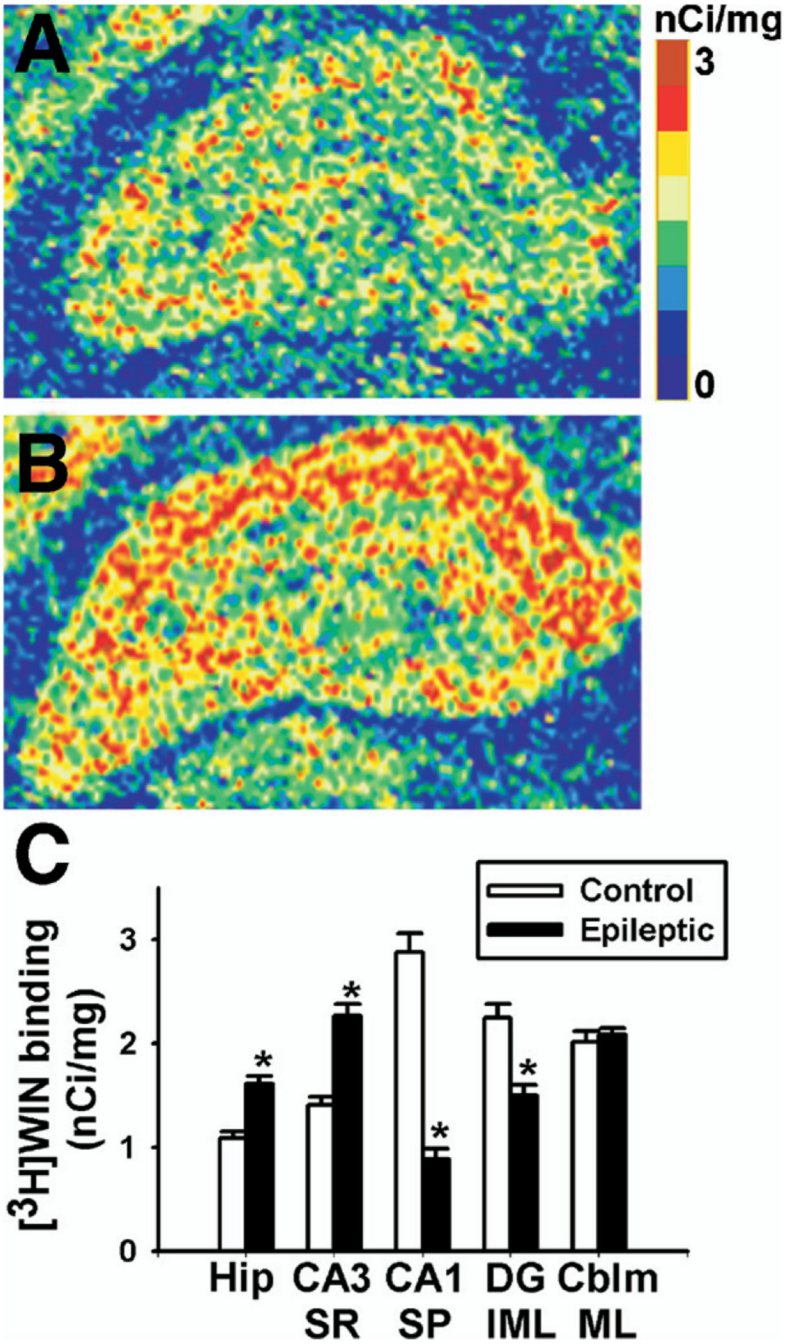

Fig. 6.

Specific [^{3}H]WIN55,212-2 binding in hippocampus from control and epileptic animals. Representative pseudocolor enhanced autoradiograms of control (A) and epileptic (B) hippocampi. Similar to Fig. 1, we observed regionally selective changes in [^{3}H]WIN55,212-2 binding. In comparison to controls, epileptic animals illustrated increased binding in the strata radiatum and oriens, and decreased binding in both the pyramidal layer and the dentate gyrus inner molecular layer. The color scale bar represents [^{3}H]WIN55,212-2 binding expressed as nCi/mg, with 0 being the lowest (blue), and 3 the highest (maroon). (C) Specific [^{3}H] WIN55,212-2 binding generated from densitometric analysis in control and epileptic rats. Regions analyzed included the whole hippocampus (Hip), the stratum radiatum at CA3 (CA3

SR), the stratum pyramidale at CA1 (CA1 SP), the dentate gyrus inner molecular layer (DG IML) and the cerebellum molecular layer (CBLM ML). Epileptic animals exhibited increases in [^{3}H]WIN55,212-2 binding in both whole hippocampus and stratum radiatum, and decreases in the inner molecular layer and stratum pyramidale, without changing in the cerebellum (n=6–10 per group, Student's t-test, * P<0.0005).

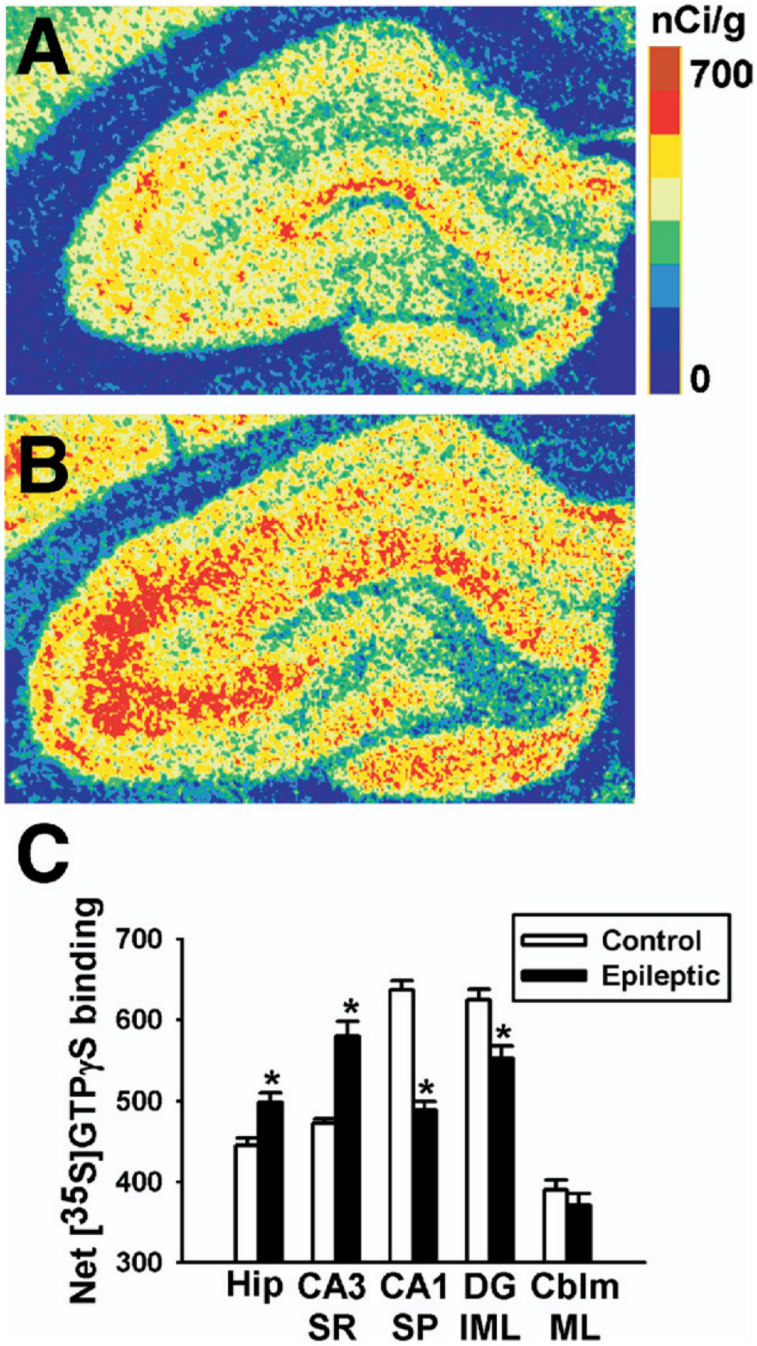

Fig. 7.

Net WIN55,212-2-stimulated [^{35}S]GTPγS binding in control and epileptic hippocampi. Representative pseudocolor autoradiograms of control (A) and epileptic (B) hippocampi. Like in Fig. 5 and Fig. 6, we observed regionally selective changes in [^{35}S]GTPγS binding. In comparison to controls, epileptic animals exhibited increased [^{35}S]GTPγS binding in the strata radiatum and oriens, and decreased [^{35}S]GTPγS binding in both the pyramidal layer and dentate gyrus inner molecular layer. The scale bar represents net [^{35}S]GTPγS binding in nCi/g, with 0 being the lowest (blue) and 700 being the highest (maroon). (C) Net WIN55,212-2-stimulated [^{35}S]GTPγS binding generated from densitometric analysis in control and epileptic rats. Regions analyzed included the whole hippocampus (Hip), the stratum radiatum at CA3 (CA3

SR), the stratum pyramidale at CA1 (CA1 SP), the dentate gyrus inner molecular layer (DG IML), and the cerebellum molecular layer (CBLM ML). Epileptic animals exhibited increases in [^{35}S]GTPγS binding in both whole hippocampus and stratum radiatum, but decreases in the dentate gyrus inner molecular layer and stratum pyramidale, without a change in the cerebellum molecular layer (n=6–10 per group, Student's t-test, * P<0.0005).

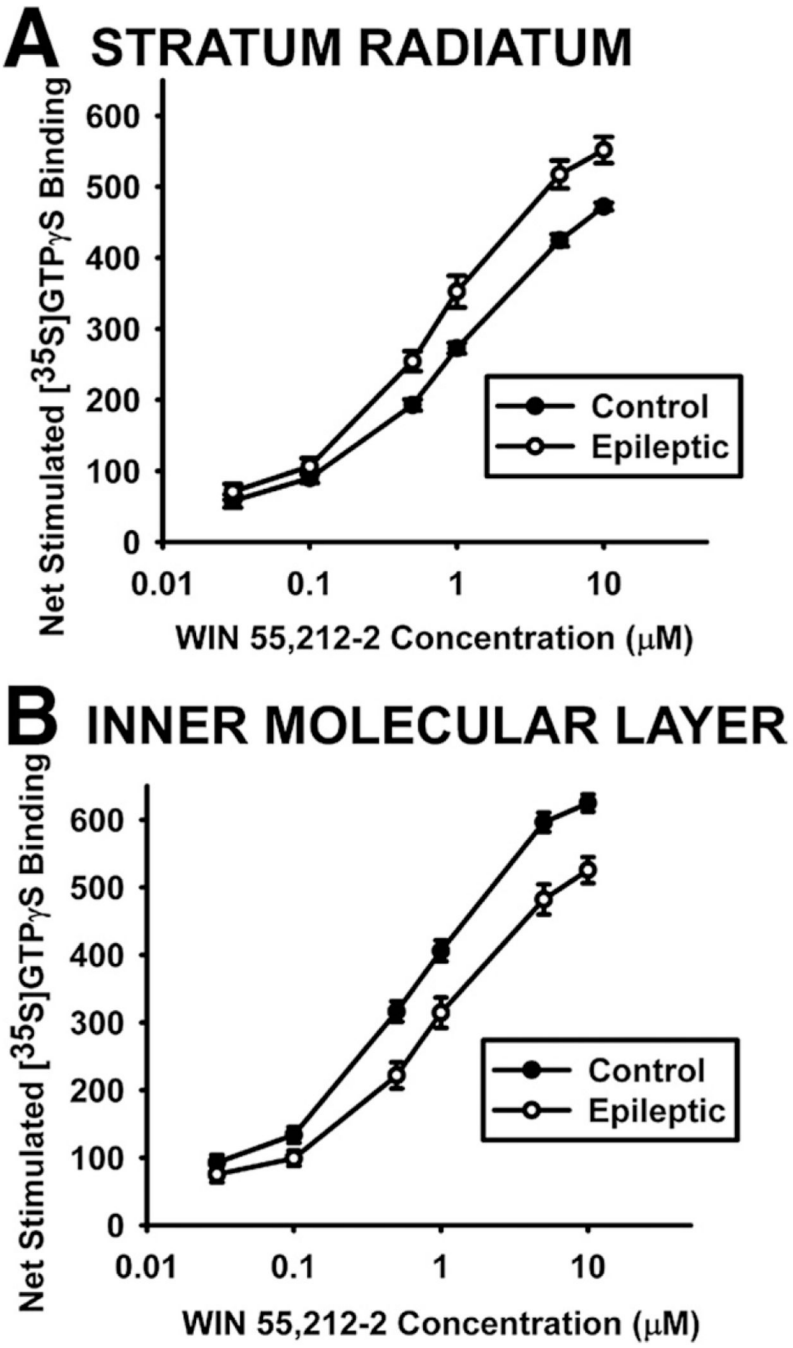

Fig. 8.

Concentration-effect curves showing mean±SEM of net WIN55,212-2-stimulated [^{35}S] GTPγS binding in brains from 10 control and 9 epileptic rats. WIN55,212-2 concentrations ranged from 0.03 μM to 10 μM in brain sections analyzed in the stratum radiatum at CA3 (A) and in the dentate gyrus inner molecular layer (B) of the hippocampus. The E_{max} and EC_{50} values generated from these curves are shown in Table 2.

Table 1

Net agonist-stimulated [^{35}S]GTPγS binding in control and epileptic animals

Treatment	Whole hippocampus		Stratum radiatum		Inner molecular layer	
	Control	Epileptic	Control	Epileptic	Control	Epileptic
WIN55,212-2	204±9	242±13*	250±11	318±15*	275±13	252±15
SR141716A	1±6	−4±9	2±5	3±8	−12±5	−5±11
WIN+SR	−1±7	−3±6	2±6	11±8	−6±7	−9±7
WIN55,212-2	490±15	542±15*	541±15	604±18*	628±11	549±26*
CP55,940	469±8	516±9*	519±8	570±15*	627±13	555±22*
MethAEA	216±10	267±10*	245±13	311±17*	320±13	283±18
WIN55,212-2	412±11	443±36	515±12	632±14*	572±20	502±17*
PIA	459±19	497±16	581±20	622±30	441±25	473±31
Baclofen	66±5	78±11	73±8	104±11*	61±14	88±3
S1P	506±19	541±15	623±22	695±21	534±20	552±25
DAMGO	117±10	117±11	139±10	129±8	154±21	156±27

Data represent mean±SEM of net agonist-stimulated [^{35}S]GTPγS binding (nCi/g) from three separate assays for maximally effective concentrations of several cannabinoid and non-cannabinoid G-protein-coupled receptor agonists, as well as in the presence or absence of cannabinoid CB1 receptor antagonist SR141716A (n=8–10 per group, unpaired Student's t-test).

*P<0.05.

Table 2

Calculated E_{max} and EC_{50} values for WIN55,212-2-stimulated [^{35}S]GTPγS binding in control and epileptic animals

Brain region	Treatment	EC_{50}, μM	E_{max}, nCi/g
Whole hippocampus	Control	0.76±0.07	470±7
	Epileptic	0.71±0.08	501±12*
Stratum radiatum	Control	0.75±0.06	496±7
	Epileptic	0.62±0.06	579±16**
Inner molecular layer	Control	0.52±0.05	650±10
	Epileptic	0.76±0.11*	554±15**

Differences in the potency and in the maximal effect of WIN55,212-2 in stimulating [^{35}S]GTPγS binding were evaluated using concentration-effect curves from control and epileptic brains slices containing hippocampus. Within the hippocampus, the stratum radiatum at CA3 and the inner molecular layer of the dentate gyrus were also quantitated. EC_{50} and E_{max} values were calculated from individual concentration effect curves generated for each rat. Values represent the mean±SEM from 9 to 10 animals per treatment group (unpaired Student's *t*-test).

* $P<0.05$ when compared to control.

** $P<0.001$ when compared to control.